Surface behavior of apolipoprotein A-I and its deletion mutants at model lipoprotein interfaces

Libo Wang, Xiaohu Mei, David Atkinson and Donald M. Small[1]

Department of Physiology and Biophysics, Boston University School of Medicine, Boston, MA 02118

Abstract Apolipoprotein A-I (apoA-I) has a great conformational flexibility to exist in lipid-free, lipid-poor, and lipid-bound states during lipid metabolism. To address the lipid binding and the dynamic desorption behavior of apoA-I at lipoprotein surfaces, apoA-I, Δ(185-243)apoA-I, and Δ(1-59)(185-243)apoA-I were studied at triolein/water and phosphatidylcholine/triolein/water interfaces with special attention to surface pressure. All three proteins are surface active to both interfaces lowering the interfacial tension and thus increasing the surface pressure to modify the interfaces. Δ(185-243)apoA-I adsorbs much more slowly and lowers the interfacial tension less than full-length apoA-I, confirming that the C-terminal domain (residues 185-243) initiates the lipid binding. Δ(1-59)(185-243)apoA-I binds more rapidly and lowers the interfacial tension more than Δ(185-243)apoA-I, suggesting that destabilizing the N-terminal α-helical bundle (residues 1-185) restores lipid binding. The three proteins desorb from both interfaces at different surface pressures revealing that different domains of apoA-I possess different lipid affinity. Δ(1-59)(185-243)apoA-I desorbs at lower pressures compared with apoA-I and Δ(185-243) apoA-I indicating that it is missing a strong lipid association motif. We propose that during lipoprotein remodeling, surface pressure mediates the adsorption and partial or full desorption of apoA-I allowing it to exchange among different lipoproteins and adopt various conformations to facilitate its multiple functions.—Wang, L., X. Mei, D. Atkinson, and D. M. Small. **Surface behavior of apolipoprotein A-I and its deletion mutants at model lipoprotein interfaces.** *J. Lipid Res.* **2014.** 55: 478–492.

Supplementary key words lipid binding • adsorption and desorption • conformational flexibility • lipid association motif • lipid affinity • interfacial tension • surface pressure • triolein/water interface • phosphatidylcholine/triolein/water interface

Apolipoprotein A-I (apoA-I) is a major protein of high density lipoproteins (HDLs) and is also present on large triacylglycerol (TAG)-rich lipoproteins. Reduced plasma levels of HDL and apoA-I are the key risk factors for atherosclerosis and cardiovascular disease (1). The anti-atherogenic properties of apoA-I arise primarily through its important roles in the pathway of reverse cholesterol transport; where apoA-I stabilizes and maintains the structure of HDL particles, promotes cellular cholesterol efflux by binding to specific ATP binding cassette transporters, interacts with the enzyme lecithin:cholesterol acyltransferase (LCAT) to drive the maturation of HDL particles, binds and modifies the lipoprotein surface to facilitate enzyme reactions, and interacts with the scavenger receptor class B type 1 for selective cholesterol ester (CE) uptake by the liver for excretion (2–4).

ApoA-I exists in lipid-free, lipid-poor, and lipid-bound states in plasma, and exchanges among HDL and TAG-rich lipoprotein particles like very low density lipoproteins (VLDLs) and chylomicrons (CMs) (5). ApoA-I interacts primarily with the hydrocarbon chains of the phospholipids (PL) on discoidal and spherical HDLs (6–8) and may also interact with the hydrophobic CE core of spherical HDL and the hydrophobic TAG core of TAG-rich lipoproteins. The conformational flexibility of apoA-I allows it to adopt a variety of conformations involving lipid adsorption, partial or full desorption, and flexible unfolding and refolding in diverse physical environments to facilitate its multiple functions. Studies of the molecular mechanisms of the lipid association and the conformational flexibility of apoA-I are essential for understanding the structure-function relationships.

ApoA-I has an exon 3 encoded region (residues 1-43), and an exon 4 encoded region (residues 44-243) that contains 10 11/22-mer tandem repeat amino acid segments that are predicted to form class A and class Y amphipathic α-helices (AαHs) (9, 10). These AαHs (helix 1-10) are the lipid binding motif of apoA-I and the structural basis for its multiple functions. Segment deletion and point mutation studies have elucidated the possible conformation and functions for each helical segment (11–16). Several studies have suggested that the lipid-free apoA-I molecule possesses a

Abbreviations: AαH, amphipathic α-helix; ANS, 1-anilinonaphthalene-8-sulfonate; A/W, air/water; CE, cholesterol ester; CM, chylomicron; POPC, phosphatidylcholine; PL, phospholipid; SUV, small unilamellar vesicle; TAG, triacylglycerol; TO, triolein; TO/W, triolein/water.

[1] To whom correspondence should be addressed.
   e-mail: dmsmall@bu.edu

two domain structure with a more rigid N-terminal α-helix bundle domain and a less organized C-terminal domain (11, 15, 17, 18). The recent advance in solving the 2.2 Å crystal structure of a truncated apoA-I mutant, Δ(185-243) apoA-I dimer, suggests that residues 1-184 independently fold in a four helix bundle and residues 185-243 form a less organized C-terminal domain in solution (19). In the crystal, the N-terminal sub-domain encompassing residues 1-43 forms a helix bundle with helix 1 (residues 44-65) and helix 2-4 (residues 66-120) from one Δ(185-243)apoA-I molecule, and helix 6-7 (residues 143-184) from the other Δ(185-243) apoA-I molecule. The authors reinforce the suggestion that the N-terminal 1-43 residues stabilize the apoA-I structure by forming a stable helix bundle.

The interactions of apoA-I with PL or lipid emulsions containing a hydrophobic core (TAG or CE) and a PL surface (5, 20–26) have been widely investigated to understand how apoA-I behaves at lipoprotein surfaces. Deletion mutations (11–14, 17), synthetic peptides encompassing specific regions (27–29), and consensus peptides of apoA-I (30) have been used to determine the lipid affinity of different segments of apoA-I. Such studies suggest that different parts of apoA-I might bind with different affinity to lipid or lipoprotein surfaces (18, 31). The C-terminal region (residues 185-243) has the highest affinity for PL and plays a critical role in initiating the lipid binding (11, 18, 31–33), while the N-terminal region (residues 1-43) has a moderate PL-binding ability (28, 34) and is thought to stabilize the lipid-free apoA-I conformation (16, 19). The hydrophobicity of the C-terminal residues 220-243 modulates the lipid binding of apoA-I, while mutations in the N-terminal 1-43 residues also play a role (35). When bound to lipoproteins of different size, the apoA-I molecule adjusts its conformation by extruding some segments into the aqueous phase (36–38). Hydrogen exchange and mass spectrometry studies showed that 20% more residues of apoA-I are forced off a small discoidal HDL particle (7.8 nm) than a larger HDL particle (9.6 nm), due to the increased packing density in the small HDL (37). We also found that part of the apoA-I molecule desorbs from a model lipoprotein surface at lower pressure, while the entire molecule desorbs at much higher pressure (38). However, because of the lack of appropriate research approaches, the dynamic desorption of apoA-I is not well elucidated. Neither the location within the apoA-I molecule nor the precise nature of the desorbed segments are well established.

The surface pressure changes of lipoproteins are very important factors for the conformational flexibility of apoA-I. During lipoprotein metabolism, lipoprotein particles constantly change in size, shape, and composition due to enzyme reactions and lipoprotein remodeling activities. For example, LCAT reactions with large discoidal HDL produce CE which migrates to the core turning the discoidal particle into a spherical particle (39). Lipolytic actions produce fatty acids from PL and TAG resulting in shrinking of the particle size. Hepatic lipase reactions release free apoA-I into plasma. Lipid transfer proteins move CE, TAG, and PL molecules among HDL and TAG-rich lipoproteins resulting in changes in the particles' size and the release of free apoA-I

(40, 41). We postulate that the surface pressure changes must occur throughout the lipoprotein remodeling processes, increasing if surface-active molecules are added to the surface or core lipid molecules are depleted, which leads to partial or full desorption of apoA-I molecules and vice versa. As a result, the coverage of apoA-I on the surface probably changes as well, and so does the surface conformation. We hypothesize that during lipoprotein remodeling, surface pressure-mediated adsorption and partial or full desorption allow apoA-I to adopt different conformations to facilitate its functions and to exchange among lipoproteins. Further insight into the dynamic adsorption, desorption, and the structural flexibility of different segments of apoA-I and their relation to surface pressure will lead to a more detailed understanding of the structural basis underlying its multiple functions.

PL vesicles and lipid emulsions have been used as model systems to study the lipid binding of apoA-I molecules (5, 18, 22, 24, 25, 31). The PL vesicle model systems give information about the kinetics of the lipid-protein interaction and the type of particle formed, while the model emulsion systems have the advantage that they contain core lipids (e.g., TAG or CE) as well as surface PL molecules. However, surface pressure changes are difficult to estimate in emulsion systems (42). PL monolayers spread at an air/water (A/W) interface have been explored as a unique model system to study the pressure-mediated penetration of apolipoproteins and the segments to PL monolayers (27, 43–50). The exclusion pressure (Π_e), i.e., the surface pressure above which the protein or peptide cannot penetrate into the PL monolayer, has been used to compare the lipid affinity of the proteins or peptides. Synthesized peptides containing the 22-mer tandem repeat AαH sequences of the 44-65 and 220-241 residues of apoA-I exhibit higher Π_e values, while peptides containing the 22-mer tandem repeat AαH sequences in the central region of apoA-I exhibit lower Π_e values, indicating a relatively lower lipid affinity (27).

We have been using a novel surface chemistry technique, oil-drop tensiometry, to study the pressure-mediated adsorption, desorption, and flexibility behavior of apolipoproteins, their segments, and consensus peptides at physiologically relevant model lipoprotein surfaces (38, 51–62), such as triolein/water (TO/W) and phosphatidylcholine/triolein/water (POPC/TO/W) interfaces. Our novel technique provides a unique point of view to look at the interaction between apolipoproteins and lipids. Our previous studies (38, 58) have shown that apoA-1, a consensus AαH peptide, and two peptides encompassing residues 1-44 and 198-243 all have the lipid binding ability to modify the TO/W interface and lower the interfacial tension (γ). They desorb from the interface when compressed and readsorb when the surface is expanded. Part of apoA-1 is pushed off the interface at a pressure of ∼15 mN/m and the entire protein is expelled above ∼19 mN/m. The full-length apoA-I molecule is elastic and very flexible, but not the short peptides. The (1-44)apoA-I peptide binds less strongly than the (198-243)apoA-I peptide at both the TO/W and the POPC/TO/W interfaces (53, 58). These results suggest that the surface pressure-mediated desorption and readsorption,

and the conformational flexibility of apoA-I probably provide lipoprotein stability during metabolic remodeling reactions in plasma.

In the present paper we have continued our surface study on the full-length apoA-I and two deletion mutants of apoA-I, Δ(185-243)apoA-I and Δ(1-59)(185-243)apoA-I, on both the TO/W and the POPC/TO/W interface. We have measured and compared the adsorption isotherms, desorption on compression, and the readsorption on expansion of these proteins. Such information may help to determine the surface behaviors of different apoA-I domains on lipoprotein surfaces and the conformational changes that might occur in apoA-I during lipoprotein remodeling, and lead to a better understanding of the molecular mechanisms underlying the multiple functions of apoA-I during reverse cholesterol transport and lipid metabolism.

EXPERIMENTAL PROCEDURES

Materials

Two deletion mutations of apoA-I, Δ(185-243)apoA-I and Δ(1-59)(185-243)apoA-I were expressed in *Escherichia coli* BL21(DE3) CodonPlus-RIL (Stratagene) cells using a His$_6$-MBP-TEV expression system and purified as described previously (19). The proteins contained an extra glycine at the N terminus derived from the TEV cleavage site. Freshly purified mutants in PBS buffer were divided into small aliquots, rapidly frozen in liquid nitrogen, and stored at −80°C. A protein aliquot was thawed before the interfacial study and stored in a refrigerator for short term storage. Both mutants were over 95% in purity by SDS-PAGE gels. Plasma apoA-I was isolated and purified as previously described (63), and characterized by SDS-PAGE gel and circular dichroism spectroscopy. The protein concentration was determined by Lowry protein assay.

For interfacial studies, varied amounts of apoA-I (1–3 mg/ml), Δ(185-243)apoA-I (1–1.5 mg/ml), or Δ(1-59)(185-243)apoA-I (0.5–1 mg/ml) were added to the aqueous phase surrounding a TO drop or a POPC-coated TO drop to obtain different aqueous phase concentrations for the three proteins, ranging from 1 × 10^{-8} M to 3 × 10^{-6} M, respectively. The pH of the aqueous phase was kept at pH 7.4 with phosphate buffer (2 mM).

TO (>99% pure) was purchased from Nu-Chek Prep, Inc. (Elysian, MN) and its interfacial tension was determined to be ∼32 mN/m at 25.0 ± 0.1°C. POPC was purchased from Avanti Polar Lipids (Alabaster, AL) in chloroform at 25 mg/ml. All other reagents were of analytical grade.

Small unilamellar vesicles (SUVs) of POPC were prepared according to the following protocol. First the lipid was dried by evaporating the chloroform using a jet of nitrogen, and then the dried lipid film was suspended in PBS buffer to a concentration of 2.5–5 mg/ml. The turbid suspension was sonicated using a probe sonicator for about 1 h with a pulsed duty cycle of 30%. The final suspension was virtually clear with the particle sizes in the range of 21–28 nm as monitored by electron microscopy.

Interfacial tension measurement

The γ of the TO/W or the POPC/TO/W interface in the presence of different amounts of apoA-I, Δ(185-243)apoA-I, or Δ(1-59)(185-243)apoA-I in the aqueous phase [2 mM (pH 7.4) phosphate buffer] was measured with an I. T. Concept Tracker

oil-drop tensiometer (Longessaigne, France) (64). To measure the γ of the TO/W interface, a 16 μl TO drop was formed in a cuvette containing 6 ml aqueous phase with a given amount of proteins and γ was recorded continuously until it reached equilibrium.

To measure the γ of the POPC/TO/W interface, a 16 μl TO drop was formed in 6 ml aqueous phase containing 200 μl POPC SUV stock (2.5–5 mg/ml) and γ was recorded continuously. POPC molecules adsorbed onto the TO drop and lowered the γ. When γ reached ∼25 mN/m, the excess POPC SUVs in the aqueous phase were removed by the buffer exchange procedure (see following method) and γ stayed constant. When γ was about 25 mN/m, the coverage of POPC on the interface was about 37% (65). Then different amounts of protein stocks were added to the aqueous phase to obtain different protein concentrations. The γ of the POPC/TO/W interface was continuously recorded until it reached equilibrium. All experiments were carried out at 25 ± 0.1°C in a thermostated system with gentle stirring.

Buffer exchange procedure

We exchanged the aqueous phase (6 ml) containing either POPC or protein with fresh buffer by continuously removing the aqueous phase from the surface and infusing fresh buffer near the bottom of the stirred cuvette. Approximately 250 ml or 150 ml of fresh buffer was exchanged for removing POPC or proteins, respectively. These exchange volumes removed more than 99.9% of the POPC or the proteins in the aqueous phase (65). POPC once adsorbed on the TO/W interface does not desorb, so γ does not change while removing POPC SUVs. While removing excess proteins, if bound protein desorbs into the aqueous phase during or after the buffer exchange the surface concentration will fall and γ will rise.

Setting the initial surface pressure and the surface concentration of POPC at POPC/TO/W interface

Different surface concentrations of POPC (Γ_{POPC}) at the POPC/TO/W interface were set by either expanding or compressing the interface, i.e., decreasing or increasing the surface pressure (Π). First, POPC SUVs were added to the aqueous phase and adsorbed onto the TO/W interface. Once γ reached 25 mN/m excess, POPC vesicles were removed from the aqueous phase by the buffer exchange procedure. Because POPC does not desorb from the interface, the amount of POPC on the surface remained the same (∼37% coverage). When the interface was expanded, the surface area increased so the Γ_{POPC} and the Π decreased. When the interface was compressed, the surface area decreased, thus the Γ_{POPC} and the Π increased. The expansion or compression was stopped when Π reached the target value, i.e., initial surface pressure (Π_i). The bigger the Π_i was, the greater the Γ_{POPC} was (65). An example of adjusting the Γ_{POPC} to a lower level by expanding the interface is shown in the left part of the plots in Fig. 3A, before the second buffer exchange.

Penetration of the proteins into the POPC/TO/W interface and the measurement of the exclusion pressure

Exclusion pressure (Π_{EX}) refers to the pressure above which a protein cannot penetrate into the POPC/TO/W interface. First, the TO drop (16 μl) was coated with POPC until γ reached ∼25 mN/m, and the excess POPC vesicles were removed from the aqueous phase. Then, the Γ_{POPC} and Π_i were set by either compressing or expanding the interface. Finally an aliquot of protein stock was added to the aqueous phase. We kept the final concentration of each protein at about 6 × 10^{-8} M. Upon addition of the protein, γ fell toward equilibrium. The general procedure is shown in Fig. 2A, from the beginning until the start of the second buffer exchange shown by the second bar. The fall (change) of the surface tension (Δγ) was measured and it varied at different

Π_is. To derive the Π_{EX} value, $\Delta\gamma$ was plotted against Π_i and the data were fit to a straight line. The intercept of the straight line at $\Delta\gamma = 0$ gave the Π_{EX} at which the protein could not penetrate into the POPC/TO/W interface (Fig. 2B).

Instant compression and expansion of the TO/W interface and the maximum pressure at which protein remains on the interface

Instantaneous compression and expansion experiments were conducted before and after the buffer exchange procedure to evaluate the desorption and readsorption behavior of bound proteins at the TO/W interface. Upon the addition of proteins to the aqueous phase, γ fell to approach an equilibrium level. After that, the TO drop (16 μl) was compressed by suddenly decreasing the volume by a different percent of the original volume (6–75%). The compressed volume was held constant for several minutes and γ was recorded continuously. The sudden decrease in drop volume instantaneously decreased the drop surface area and resulted in a sudden compression causing γ to drop abruptly to a certain level, γ_0. The surface pressure generated at instant compression (Π_0) = $\gamma_{TO} - \gamma_0$, where γ_{TO} is the surface tension of pure TO (32 mN/m). If bound protein or regions of the protein readily desorb from the surface upon compression, γ will rise toward a new equilibrium value (desorption curve). If the protein does not desorb the γ will remain constant at the same level as γ_0 (56). The compressed surface was reexpanded by increasing the drop volume back to the original volume (16 μl) and held constant for several minutes. The changes in γ following the reexpansion (readsorption curve) may depend on whether there is protein in the aqueous phase (before buffer exchange) or the protein has been removed (after buffer exchange). In either case, γ will rise promptly after reexpansion because the surface concentration decreases as the surface area increases. Before protein removal, if bound protein desorbs upon compression, the reexpansion will provide new space for protein in the aqueous phase to readsorb to the surface and γ will fall back to the original equilibrium. After the protein removal, the changes of γ will follow one of two paths upon reexpansion. If protein desorbs on compression, γ will rise to a higher level than the original equilibrium and remain constant, because there is virtually no protein in the aqueous phase to readsorb. On the other hand, if protein is only partially desorbed but still attached to the surface on compression, upon expansion the ejected part will readsorb onto the surface and γ will fall back to the original equilibrium with faster kinetics (38). For a demonstration of the protocol, refer to Fig. 4A–C. To estimate the maximum surface pressure (Π_{MAX}) that protein could withstand without being ejected from the interface, a series of instant compression and expansion experiments at different ratios over a wide range of protein concentrations were carried out. The $\Delta\gamma$s over the compression period were plotted against the Π_0 and the data were fit to a straight line. The intercept at $\Delta\gamma = 0$ gave the Π_{MAX} at which the protein molecules showed no net adsorption or desorption (38).

Slow compression and expansion of the interface and pressure/area isotherms

Slow compressions and expansions of the TO/W and POPC/TO/W interfaces were conducted after the buffer exchange procedure. For the POPC/TO/W interface, a Π_i was set before adding protein, with a similar protocol for the Π_{EX} measurement. The typical procedure was as follows. A certain amount of protein ($\sim$5.4–5.8 $\times$ 10^{-8} M) was added to the aqueous phase surrounding the interface, and γ was continuously recorded until it reached equilibrium. Then the protein in the aqueous phase was removed by buffer exchange. After the tension had equilibrated, the interface was slowly expanded at a linear rate of 0.02 μl/s toward a volume in the range of 25–30 μl. As the surface was expanded, the

surface concentration decreased and the surface pressure fell. After the interface had equilibrated for a short period of time, the interface was slowly compressed at a linear rate of 0.02 μl/s toward a very small volume or until the drop was lost. See Fig. 3A for the demonstration of the general protocol. A surface pressure against area (Π-A) curve derived from the compression procedure (examples in Fig. 5) showed the desorption details of the proteins. The pressure at which the Π-A curve changes slope is called the envelope pressure, Π_E. Usually, Π_E is the pressure when part of the protein or the whole protein molecule is ejected from the surface. By examining the shape and the Π_E of the Π-A curves, detailed desorption information of the proteins from either the POPC/TO/W interface or TO/W interface was derived.

RESULTS

Adsorption of apoA-I, Δ(1-59)(185-243)apoA-I, and Δ(185-243)apoA-I on the TO/W and the POPC/TO/W interfaces: apoA-I and Δ(1-59)(185-243)apoA-I bind more rapidly and strongly

We have shown the adsorption isotherms of apoA-I at the TO/W interface previously (38). Now we report the adsorption behavior of Δ(1-59)(185-243)apoA-I and Δ(185-243) apoA-I on the TO/W interface. Adsorption curves at varied protein concentrations in the range of 10^{-8}–10^{-6} M for each protein were measured. Examples are shown in **Fig. 1A**. Plots of the equilibrium γ against the natural log of the protein concentration show the different adsorption behavior of the three proteins (Fig. 1B). Like full-length apoA-I, both apoA-I truncated mutants are surface active and lowered the γ of the TO/W interface (32 mN/m) to reach an equilibrium level. The equilibrium γ is dependent on the protein concentration in the aqueous phase (Fig. 1B). In general, higher protein concentrations resulted in lower γ at equilibrium, and less time to reach the equilibrium. At similar protein concentrations, full-length apoA-I and Δ(1-59)(185-243)apoA-I lowered the γ of the TO/W interface to almost the same level, while Δ(185-243)apoA-I lowered the γ much less (Fig. 1B). Δ(185-243)apoA-I also needed a much longer time to reach equilibrium (data not shown). For example, at a protein concentration of $\sim$4 $\times$ 10^{-7} M, the γ of the TO/W interface was lowered to 15.4 mN/m with apoA-I and 15.1 mN/m with Δ(1-59)(185-243)apoA-I, while Δ(185-243)apoA-I γ was lowered to 19.6 mN/m. At relatively similar concentrations in the range of 3–4 $\times$ 10^{-7} M, the half time needed to reach equilibrium was 100 s for apoA-I, 94 s for Δ(1-59)(185-243)apoA-I, and 320 s for Δ(185-243)apoA-I. These data indicate that Δ(185-243)apoA-I has a lower lipid binding ability to the TO/W interface.

The adsorption isotherms of the three proteins at the POPC/TO/W interface were measured with a POPC/TO/W interface tension of 25 mN/m, i.e., $\sim$37% coverage of POPC (65). The protein concentrations in the aqueous phase were in the range of 3–1.5 $\times$ 10^{-6} M. Examples of the adsorption curves are shown in Fig. 1C. The equilibrium γ versus the natural log of the protein concentration plots of the three proteins are shown in Fig. 1D. Similar to the adsorption to the TO/W interface, all three proteins bound and lowered the γ of the POPC/TO/W interface
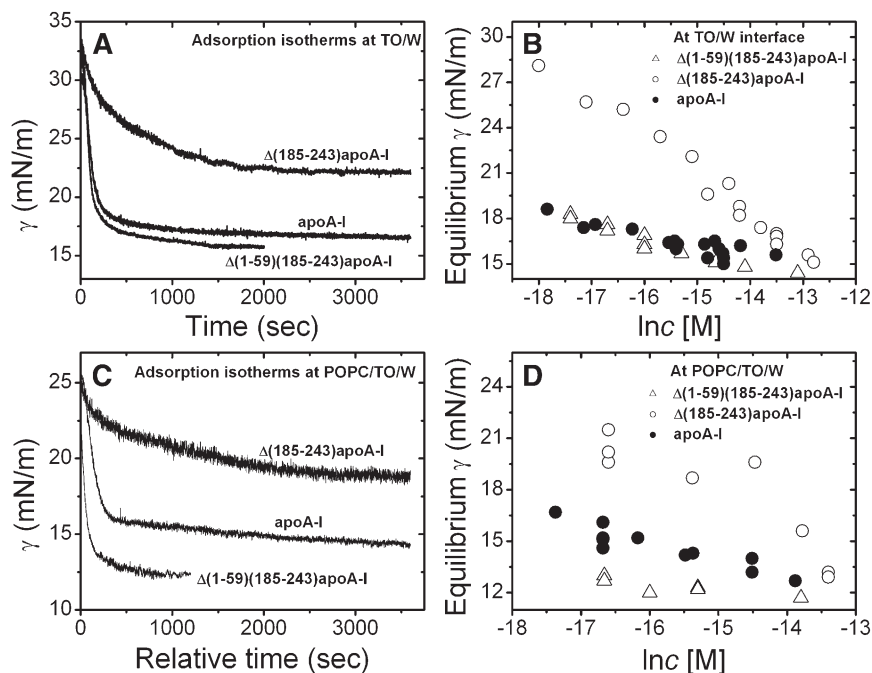
Fig. 1. A: Examples of the adsorption isotherms at the TO/W interface. $\Delta(1\text{-}59)(185\text{-}243)$apoA-I ($2.3 \times 10^{-7}$ M), $\Delta(185\text{-}243)$apoA-I (3.1×10^{-7} M), and apoA-I (3.3×10^{-7} M) in the aqueous phase (2 mM, pH 7.4, phosphate buffer). B: The equilibrium γ against natural log of the protein concentration plots at the TO/W interface. Open triangle, $\Delta(1\text{-}59)(185\text{-}243)$apoA-I; open circle, $\Delta(185\text{-}243)$apoA-I; solid circle, apoA-I. C: Examples of the adsorption isotherms at the POPC/TO/W interface. $\Delta(1\text{-}59)(185\text{-}243)$apoA-I ($2.3 \times 10^{-7}$ M), $\Delta(185\text{-}243)$apoA-I (2.1×10^{-7} M), and apoA-I (1.7×10^{-7} M) in the aqueous phase (2 mM, pH 7.4, phosphate buffer). D: The equilibrium γ against natural log of the protein concentration plots at the POPC/TO/W interface. Open triangle, $\Delta(1\text{-}59)(185\text{-}243)$apoA-I; open circle, $\Delta(185\text{-}243)$apoA-I; solid circle, apoA-I.

from ~25 mN/m to an equilibrium level. Higher protein concentrations resulted in lower γ at equilibrium, and less time to reach the equilibrium. The full-length apoA-I and $\Delta(1\text{-}59)(185\text{-}243)$apoA-I lowered the γ to a lower equilibrium level compared with $\Delta(185\text{-}243)$apoA-I, and with a slightly faster rate (data not shown). For instance, at the protein concentration of ~6×10^{-8} M, γ was lowered to ~13 mN/m with $\Delta(1\text{-}59)(185\text{-}243)$apoA-I, to ~15.3 mN/m with full-length apoA-I, and to ~20.4 mN/m with $\Delta(185\text{-}243)$apoA-I. The corresponding half time toward the equilibrium was 195 s for $\Delta(1\text{-}59)(185\text{-}243)$apoA-I, 332 s for apoA-I, and 405 s for $\Delta(185\text{-}243)$apoA-I. Thus $\Delta(185\text{-}243)$apoA-I has the weakest lipid binding ability to the POPC/TO/W interface among the three proteins.

Penetration of apoA-I, $\Delta(1\text{-}59)(185\text{-}243)$apoA-I, and $\Delta(185\text{-}243)$apoA-I into the POPC/TO/W interface and the Π_{EX}: $\Delta(185\text{-}243)$apoA-I is more stable in solution than on the lipid interface

To compare and quantify the penetration behavior at the POPC/TO/W interface, we measured the Π_{EX} of each protein. **Figure 2A** shows an example of measuring the Π_{EX} data of $\Delta(1\text{-}59)(185\text{-}243)$apoA-I. Starting with a POPC/TO/W interface with a tension at around 25 mN/m, the excess POPC vesicles were removed from the aqueous phase by buffer exchange (shown by the bar at left). The γ was then adjusted to ~27.6 mN/m (setting the Π_i) by expanding the interface from 29.5 mm^2 to 37.2 mm^2, i.e., the Π_i was

about 4.4 mN/m. The $\Delta(1\text{-}59)(185\text{-}243)$apoA-I was added at this point to the aqueous phase to a final concentration of ~5.4×10^{-8} M, causing γ to drop to 14.4 mN/m and a $\Delta\gamma$ of ~13.2 mN/m. A series of experiments were carried out at different Π_is with each protein. Upon addition of the proteins, the $\Delta\gamma$s were plotted against Π_i and the data were fit to a straight line. The intercept of the straight line at which $\Delta\gamma = 0$ is the Π_{EX}, the pressure above which protein cannot penetrate into the POPC/TO/W interface. Figure 2B shows the experiment data of the three proteins and the Π_{EX} values. These data suggest that apoA-I and $\Delta(1\text{-}59)(185\text{-}243)$apoA-I have strong penetration ability, with a Π_{EX} of 24.8 mN/m for $\Delta(1\text{-}59)(185\text{-}243)$apoA-I and 22.6 mN/m for apoA-I, while $\Delta(185\text{-}243)$apoA-I has a lower Π_{EX} of 20.2 mN/m, indicating a weak penetration ability in the POPC/TO/W interface. The Π_{EX} analysis is consistent with the adsorption characterization for the three proteins (Fig. 1C, D) in that both apoA-I and $\Delta(1\text{-}59)(185\text{-}243)$apoA-I have a strong tendency to adsorb or penetrate into the POPC/TO/W interface while $\Delta(185\text{-}243)$apoA-I is more stable in solution.

Desorption of bound apoA-I, $\Delta(1\text{-}59)(185\text{-}243)$apoA-I, and $\Delta(185\text{-}243)$apoA-I from the TO/W interface: $\Delta(1\text{-}59)(185\text{-}243)$apoA-I desorbs at a lower Π_{MAX}

Instant compression and expansion experiments were carried out for the three proteins, both before and after the buffer exchange procedure. An example of $\Delta(1\text{-}59)(184\text{-}243)$apoA-I is shown in **Fig. 3A**. Before buffer exchange
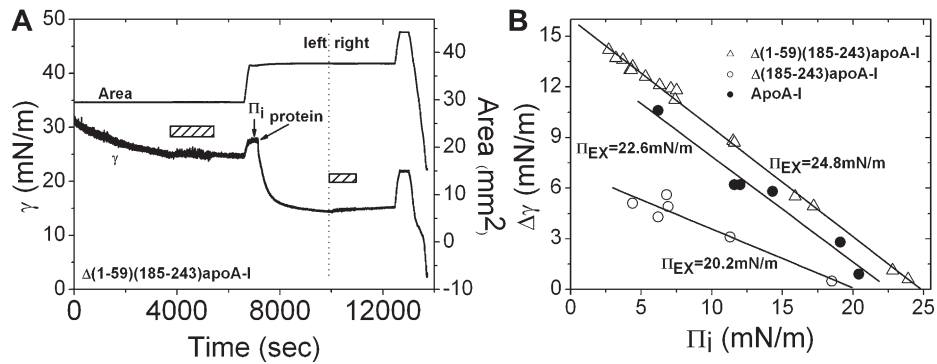
Fig. 2. An example of collecting the data for obtaining Π_{EX} (A, on the left), slow expansion and compression (A, on the right), and the Π_{EX} values at the POPC/TO/W interface (B). A: Left: A 16 µl TO drop was formed in aqueous phase containing POPC SUVs. POPC adsorbed on the TO/W interface and the γ fell. When the γ reached ~25 mN/m, excess POPC SUVs in the aqueous phase were removed by the buffer exchange (the first bar). Then the γ was adjusted to reach a Π_i of 4.4 mN/m by expanding the interface. After the interface was equilibrated, the protein $\Delta(1\text{-}59)(185\text{-}243)$apoA-I was added to the aqueous phase to obtain a concentration of 5.4×10^{-8} M and the γ fell to an equilibrium. Right: After excess protein was removed from the aqueous phase (the second bar), the interface was expanded at a linear rate of 0.02 µl/sec until the volume reached ~28.6 µl and the area was about 44.3 mm^2. The interface was then compressed at 0.02 µl/sec until Π exceeded 30 mN/m. B: The $\Delta\gamma$ upon adding the protein was plotted against Π_i at which protein was added. The data were linearly fit and the Π_{EX} values were derived (extrapolated Π_i at which $\Delta\gamma$ is zero), i.e., the Π above which protein cannot penetrate into the POPC/TO/W interface. Open triangle, $\Delta(1\text{-}59)(185\text{-}243)$apoA-I; open circle, $\Delta(185\text{-}243)$apoA-I; solid circle, apoA-I.

(shown by the bar), the area of the TO drop (~30 mm^2) was compressed at different ratios from 3% to 53% and expanded back to the original area after being compressed for several minutes. Upon compression, γ first decreased to a lower level because the instant compression increased the surface concentration immediately. Subsequently, γ rose to a new equilibrium level while the compressed area was held constant, indicating that the interfacial concentration decreased due to desorption of bound proteins from the interface. On expansion, γ first rose to a higher level because the interfacial concentration decreased when the interface was expanded. Finally, as a result of the readsorption of the free protein molecules in the aqueous

phase onto the newly generated interface, γ relaxed back to the original equilibrium level. The γ decreased more at larger compressions and rose to a higher value at corresponding expansions because the interface lost more protein compared with the smaller compressions. During the buffer exchange, little change in γ was observed indicating that $\Delta(1\text{-}59)(184\text{-}243)$apoA-I cannot be easily washed off the interface. The $\Delta(1\text{-}59)(184\text{-}243)$apoA-I and full-length apoA-I cannot be washed off the interface either (data not shown). After the buffer exchange, changes in γ on compression showed similar trends to those before the buffer exchange. However, changes in γ on expansion were different than those before buffer exchange. At the small compressions
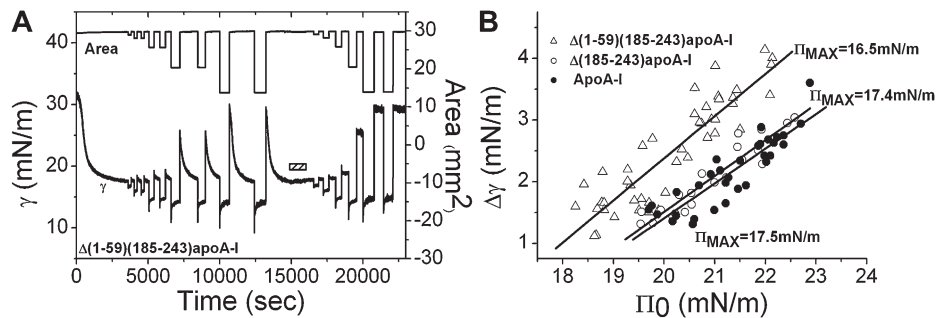

Fig. 3. A: An example of instant compression and reexpansion of $\Delta(1\text{-}59)(185\text{-}243)$apoA-I on the TO/W interface. After the protein adsorbed to the interface and reached equilibrium, the interface was rapidly compressed at different ratios (3–55% in area) and held for several minutes and then reexpanded back to the original volume (16 µl). A similar protocol was repeated after excess protein molecules were removed from the aqueous phase by buffer exchange (indicated by the bar). $\Delta(1\text{-}59)(185\text{-}243)$apoA-I is 5.4×10^{-8} M before buffer exchange. B: The Π_{MAX} values at the TO/W interface. The surface tension changes over the period when the compressed areas were held, $\Delta\gamma$s were plotted against the Πs generated at instant compressions, Π_0s. The data were linearly fit and the Π_{MAX} values for each protein were derived (extrapolated Π_0 at which $\Delta\gamma$ is zero), i.e., the maximum Π at which each protein can remain on the TO/W interface without being ejected. Open triangle, $\Delta(1\text{-}59)(185\text{-}243)$apoA-I; open circle, $\Delta(185\text{-}243)$apoA-I; solid circle, apoA-I.

of about 3–6% change in area (the first and second compressions in Fig. 3A), the γ returned to the original equilibrium level on expansion, indicating that the protein did not desorb on compression, only readjusted the conformation on expansion. On expansion after larger compressions, γ rose to a higher level than the original equilibrium and remained at that level, indicating that bound protein molecules had desorbed from the interface. Because there was no free protein in the aqueous phase after buffer exchange, no readsorption occurred and thus. the γ remained constant at the new higher level. The observation that larger compressions resulted in a higher new γ level on the subsequent expansion indicates that more protein desorbed. After several larger compressions, the new γ level was almost as high as that of an empty TO/W interface (∼30 mN/m), indicating that most of the bound protein molecules were ejected from the interface. The Δ(185-243)apoA-I and full-length apoA-I showed similar instant desorption trends as Δ(1-59)(185-243)apoA-I in that they all desorbed from the TO/W interface at specific surface pressures. As shown in Fig. 3B, apoA-I and Δ(185-243)apoA-I desorbed at very similar Π_{MAX}s of 17.5 mN/m and 17.4 mN/m, respectively, while Δ(1-59)(185-243)apoA-I desorbed at a lower Π_{MAX} of 16.5 mN/m.

Desorption of bound apoA-I, Δ(1-59)(185-243)apoA-I, and Δ(185-243)apoA-I from the POPC/TO/W interfaces: protein desorption depends on the POPC/protein ratio on the surface

Linear slow expansion and compression of the POPC/TO/W interface with bound apoA-I, Δ(1-59)(185-243)apoA-I, or Δ(185-243)apoA-I were carried out to compare the desorption behaviors. Figure 2A (on the right) shows a typical procedure of slow expansion and compression of Δ(1-59)(185-243)apoA-I. Starting with a POPC/TO/W interface (about 16 µl in volume, 30 mm^2 in area) with 37% surface coverage of POPC (about 25 mN/m in γ), excess POPC SUVs were removed from the aqueous phase and the γ was either kept at 25 mN/m or reset to a specific value by compressing or expanding the interface, i.e., setting a different Π_i. In Fig. 2A, the initial γ was set to 27.6 mN/m by expanding the interface and the Π_i was ∼4.4 mN/m. Δ(1-59)(185-243)apoA-I was added into the aqueous phase to obtain a concentration of 5.4×10^{-8} M. Once protein was bound to the POPC/TO/W interface and equilibrated, the excess protein in the aqueous phase was removed by buffer exchange, fixing the quantity of protein on the surface. The surface was then expanded at a very slow rate of 0.02 µl/s until the drop was about 25 µl. After the surface was stable, it was compressed at 0.02 µl/s until the surface pressure was over 30 mN/m. In our study, we kept the similar amount of POPC on the surface by starting with a similar POPC/TO/W interface, i.e., about 16 µl in volume, 30 mm^2 in area, and 25 mN/m in tension, and we set different Π_is by changing the area through either expanding or compressing the interface. Thus the amount of protein that adsorbed at different Π_is was different because the available interfacial area for adsorption was different. Therefore, by setting different Π_is, we were actually adjusting the POPC/protein ratios on the interface. A higher Π_i means a smaller area available for protein to adsorb, thus less protein bound and the POPC/protein ratio was larger. Π-A curves derived from the slow compression curves of the three proteins at different Π_is are shown in **Fig. 4A–C**. The inflections that show the slope changes in the Π-A curves, the Π_Es, reflect that entire proteins start to be ejected from the interface. For all three proteins, Π_E significantly increased at a higher Π_i, which corresponds to a higher POPC/protein ratio, demonstrating that it was much harder to eject the protein from the interface with a higher POPC/protein ratio. We calculated the POPC percentage coverage based on Π_i values according to the methods described previously (65), and plotted the Π_Es at different Π_is against the coverage of POPC on the interface in Fig. 4D. Figure 4 clearly shows that at larger POPC coverage, i.e., larger POPC/protein ratio, the Π_E value is higher. At similar POPC coverage, the order of the Π_Es for the three proteins is Δ(185-243)apoA-I > full-length apoA-I > Δ(1-59)(185-243)apoA-I, indicating that Δ(1-59)(185-243)apoA-I desorbs from the POPC/TO/W interface much more easily than Δ(185-243)apoA-I and apoA-I (Fig. 4D). Therefore, once bound, Δ(185-243)apoA-I and apoA-I have higher affinity for the POPC/TO/W interface. This result is consistent with the instant Π_{MAX} result at the TO/W interface, i.e., Δ(1-59)(185-243)apoA-I desorbs from the TO/W interface much more easily with a smaller Π_{MAX}.

In addition, Fig. 4D shows that the Π_Es of all three proteins at the POPC/TO/W interface are higher than the Π_Es at the TO/W interface. This result indicates that, at the POPC/TO/W interface, bound proteins interact with core lipid TO as well as with surface lipid POPC, which makes the proteins bind to the surface more strongly. This result is similar to the observation for another α-helical protein, apoC-I, which shows that it binds more strongly to the POPC/TO/W interface than the TO/W interface (52).

Sequential slow expansion and compression experiments were conducted to obtain further desorption details of the three proteins from the POPC/TO/W interface. **Figure 5A** shows an example of the sequential slow expansion and compression of Δ(1-59)(185-243)apoA-I. Instead of compressing only once until the Π approached over 30 mN/m, the interface was gradually compressed multiple times toward increased surface pressures, finally approaching ∼31 mN/m. First, protein was added into the aqueous phase surrounding a POPC/TO/W interface with a γ of ∼25 mN/m and adsorbed to the interface until γ approached equilibrium. After the excess protein was removed from the aqueous phase, the interface was expanded from 29.7 mm^2 (16 µl) to 43.5 mm^2 (28 µl) (expansion 1) and then compressed until Π reached 19.3 mN/m (compression 1). The interface was reexpanded to 43.5 mm^2 (expansion 2), and compressed further until Π was 22 mN/m (compression 2). Additional compressions to 24.2, 26.6, 27.1, and finally 29.3 mN/m and reexpansion to the original area followed. The corresponding Π-A curves for the compressions in Fig. 5A are shown in Fig. 5B. The Π-A curve for the first compression to 19.3 mN/m (black) was identical with that of the second compression to 22 mN/m (red) in the lower pressure region,
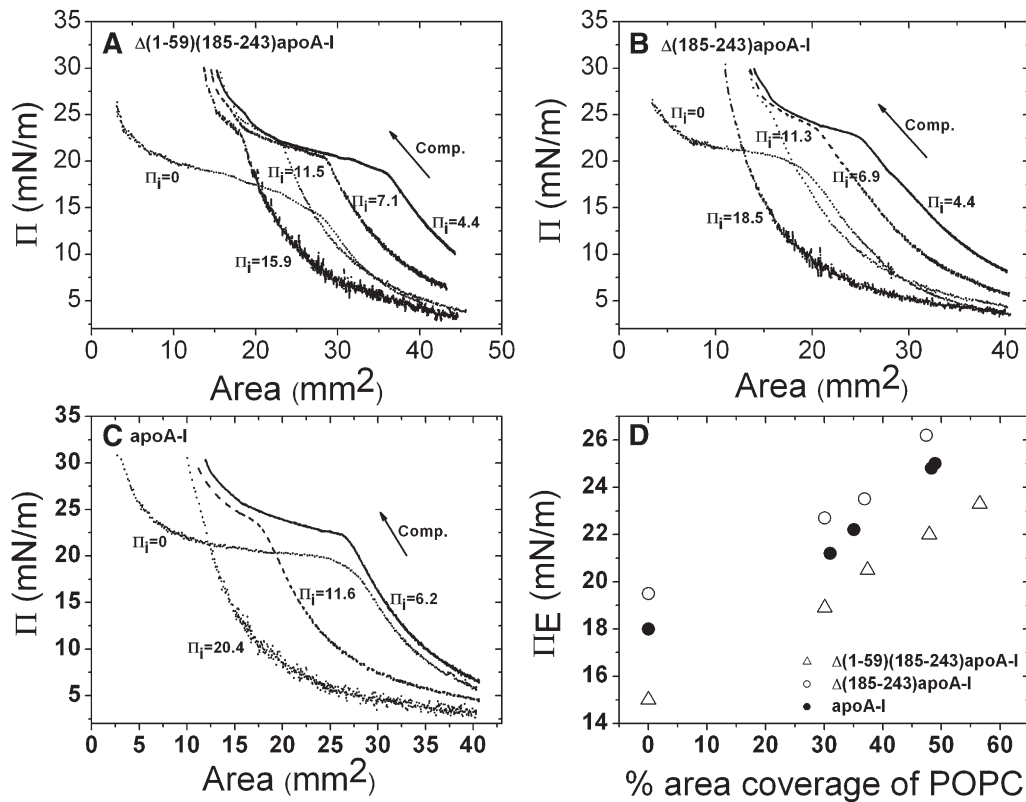
Fig. 4. Π-A curves derived from the slow compressions of Δ(1-59)(185-243)apoA-I (A), Δ(185-243)apoA-I (B), and apoA-I (C) at the POPC/TO/W interface. Typical slow compression protocol is shown in Fig. 3A. Similar slow compressions were conducted at different Π_is. At an empty TO/W interface, Π_i is 0. The compression (Comp.) is indicated by the arrow. The concentrations of Δ(1-59)(185-243)apoA-I, Δ(185-243)apoA-I, and apoA-I in the aqueous phase were 5.8×10^{-8} M, 6.1×10^{-8} M, and 5.6×10^{-8} M, respectively. D: The Π_E against the percentage area coverage of POPC plot. Π_E is the change in slope (inflection) shown in the Π-A curves. The percentage area coverage of POPC on the interface was calculated according to the method in reference (65). Open triangle, Δ(1-59)(185-243)apoA-I; open circle, Δ(185-243)apoA-I; solid circle, apoA-I.

demonstrating that nothing was pushed off at the first compression to the Π of 19.3 mN/m and that the first compression and expansion was a reversible process. During the second compression to the Π of 22 mN/m, bound Δ(1-59)(185-243)apoA-I started to desorb from the interface as shown by a sharp decrease in slope at Π_E of ~20.9 mN/m (the short arrow in Fig. 5B). When the interface was expanded back to the original area, there was less protein on the interface as shown by a higher γ (lower Π) at point c compared with points a and b in Fig. 5A. The loss of protein at compression 2 can also be seen in the Π-A curves (Fig. 5B). The starting Π of compression 3 (green line) was smaller than that of compression 2 (red line) by about 1.4 mN/m and, when the interface was compressed further, more protein was pushed off the interface as shown by higher Π_Es and smaller starting Πs of the given compressions. This result confirms that Π_E is dependent on the POPC/protein ratio on the surface. During the sequential slow compressions and expansions, increasing amounts of protein were ejected from the interface. As the amount of POPC remained the same on the interface, the POPC/protein ratio increased and the Π_E rose concomitantly. For Δ(1-59)(185-243)apoA-I, compression 5 (cyan line) to 27.1 mN/m was identical to that of compression 6 (magenta line) to 29.3 mN/m, indicating that at compression 4 (blue line) to 26.6 mN/m,

bound Δ(1-59)(185-243)apoA-I was fully ejected from the interface, so nothing could desorb during compressions 5 and 6.

Similar experiments were conducted with Δ(185-243) apoA-I and apoA-I, and Π-A curves for the compressions are shown in Fig. 5C, D. For Δ(185-243)apoA-I, the Π-A curves of the compressions to below 17 mN/m do not show Π_Es and are identical showing that bound Δ(185-243)apoA-I was not ejected from the interface at Πs below 17 mN/m. The Π-A curves of compressions to the Πs of 19.5 and 22 mN/m do not have clear Π_Es, but show some slight changes in the shape of the curves. Because the Πs of the interface after the two compressions to 19.5 and 22 mN/m had changed little from the previous compressions, we speculate that during these compressions, only small parts of the protein molecule desorbed from the interface, and that during the following expansions those connected but ejected parts readsorbed quickly. The Π-A curves of the compressions to 24.5 and 27 mN/m show that bound Δ(185-243)apoA-I desorbed at Π_Es of around 23.5 and 24.7 mN/m, respectively. However, unlike the sequential compression and expansion of Δ(1-59)(185-243) apoA-I (Fig. 5B), the Π-A curves of the compressions to 27 and 29.7 mN/m are not identical, suggesting that there was still some Δ(185-243)apoA-I on the interface at Π above
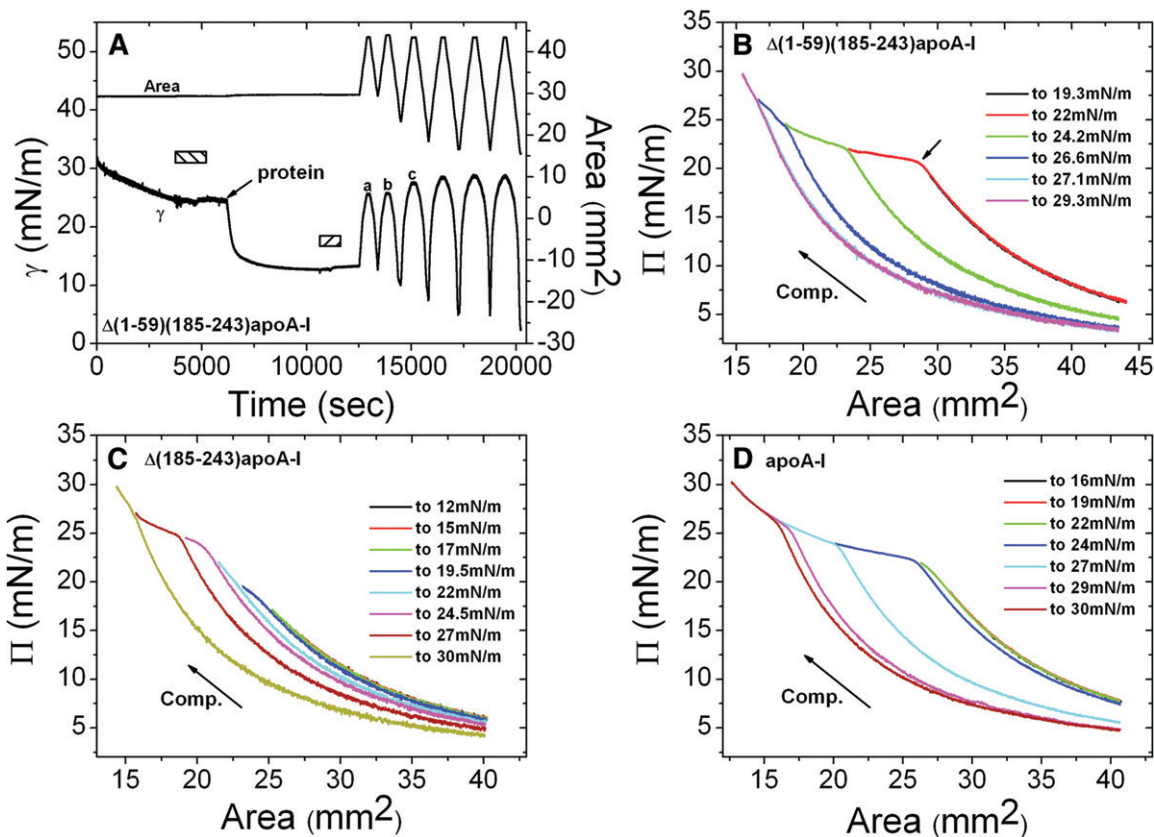
Fig. 5. An example of gradual slow compression and expansion for $\Delta(1\text{-}59)(185\text{-}243)$apoA-I (A) and Π-A curves derived from gradual compressions for $\Delta(1\text{-}59)(185\text{-}243)$apoA-I (B), $\Delta(185\text{-}243)$apoA-I (C), and apoA-I (D) at the POPC/TO/W interface. A: $\Delta(1\text{-}59)(185\text{-}243)$apoA-I was added to the aqueous phase when γ reached ~ 25 mN/m to obtain a protein concentration of 5.8×10^{-8} M. After γ reached equilibrium, excess protein molecules were removed from the aqueous phase (second bar). Then the interface was gradually expanded at a slow rate of 0.02 μl/sec until the drop volume was 28 μl and the area was about 43.5 mm^2, and then the interface was compressed at a slow rate of 0.02 μl/sec to a Π of 19.3 mN/m. The slow compression and expansion procedure was repeated to compress the interface to increasing Πs, until Π exceeded 30 mN/m. The corresponding Π-A curves for the compressions are displayed in (B). The small arrow in (B) shows the change in slope and the pressure there is the Π_E. Similar gradual expansion and compression experiments were conducted for both $\Delta(185\text{-}243)$apoA-I and apoA-I. The corresponding Π-A curves for the compressions are displayed in (C) and (D). The protein concentration was 6.1×10^{-8} M for $\Delta(185\text{-}243)$apoA-I (C) and 5.6×10^{-8} M for apoA-I (D). The compression (Comp.) is indicated by the arrow.

27 mN/m and that $\Delta(185\text{-}243)$apoA-I contains a segment with a higher lipid affinity. Similar partial desorption in the sequential compression and expansion of apoA-I is seen in Fig. 5D. Π-A curves of the compressions to 16 and 19 mN/m show reversible compressions and expansions with identical curves, and no protein desorption. During the compression to 22 mN/m, partial apoA-I was ejected from the interface but readsorbed quickly on expansion, as shown by a small shape change in the Π-A curves and a similar interfacial Π compared with that after previous compressions. Bound apoA-I was gradually pushed off the interface during compressions to Πs of 24, 27, 29, and 30 mN/m, with the Π_Es at approximately 22, 23.7, 25, and 25.6 mN/m. Even at a compression to 30 mN/m, protein was still being ejected from the interface, as shown by the small inflection, indicating that some part of apoA-I binds to the lipid interface very strongly.

Therefore, $\Delta(1\text{-}59)(185\text{-}243)$apoA-I, $\Delta(185\text{-}243)$apoA-I, and apoA-I desorb differently once bound on the POPC/TO/W surface. The $\Delta(1\text{-}59)(185\text{-}243)$apoA-I desorbs as a whole protein at relatively lower Π, while apoA-I and

$\Delta(185\text{-}243)$apoA-I both contain some high lipid affinity segments bound to the surface more tightly. Parts of the proteins desorb at lower Πs and the entire proteins desorb at much higher Πs. The maximum Π (Π_Es in this case) at which the proteins could remain on the surface without being ejected depends on the POPC/protein ratios. Less protein on the interface results in higher Π_Es, and it is harder to eject the protein. This behavior would allow some apoA-I to remain on the interface at very high pressures.

DISCUSSION

In the present paper, we studied the adsorption and desorption properties of apoA-I and its two deletion mutants, $\Delta(1\text{-}59)(185\text{-}243)$apoA-I and $\Delta(185\text{-}243)$apoA-I, at both TO/W and POPC/TO/W interfaces as a function of surface pressure. We adopted the structural model of monomeric $\Delta(185\text{-}243)$apoA-I (**Fig. 6B**) from Mei and Atkinson's (19) proposal based on the crystal structure of dimeric $\Delta(185\text{-}243)$apoA-I. In the proposed structure, an N-terminal
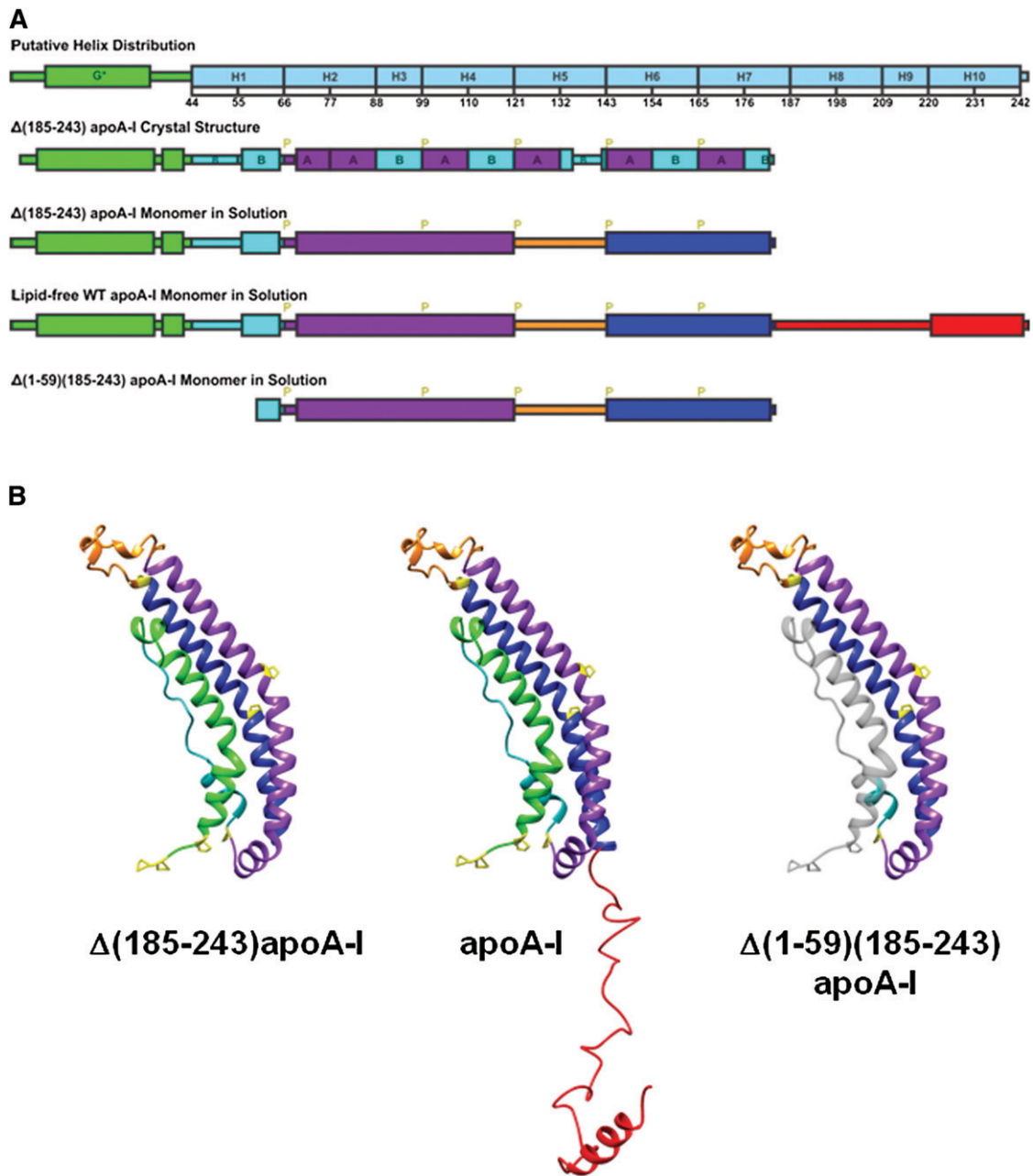
Fig. 6. A: Illustrations of the helix distribution from sequence analysis (10), Δ(185-243)apoA-I crystal structure (19), and the predicted monomer secondary structures. G*stands for the type G* AαH, H stands for the predicted Helix 1 to 10 (10), B and A stand for the B and A repeats of AαHs of apoA-I (19), and P stands for proline. B: Predicted monomer structures of Δ(185-243)apoA-I, full-length apoA-I, and Δ(1-59)(185-243)apoA-I in solution based on the crystal structure of the Δ(185-243)apoA-I dimer (19). The full-length apoA-I consists of an N-terminal α-helix bundle domain (residues 1-184), and a less organized C-terminal domain (residues 185-243). The four parts of the N-terminal α-helix bundle domain are the exon 3 encoded N-terminal region (residues 1-43, in green), helix 1 (residues 44-65, in cyan), helix 2-4 (residues 66-120, in purple), and helix 6-7 (residues 143-184, in blue), which folds back on the bundle by a hinge at helix 5 (residues 121-142, in orange). The C-terminal domain (residues 185-243, in red) extends away from the bundle and has an AαH at the end (residues 220-241). Proline residues are labeled in yellow in the monomer structures. The domain distributions are colored accordingly. The missing residues 1-59 from the Δ(1-59)(185-243)apoA-I structure are shown in gray for comparison purposes.

α-helical bundle domain (residues 1-184) consists of four segments, the exon 3 encoded N-terminal sub-domain (residues 1-43), the exon 4 encoded helix 1 (residues 44-65), helix 2-4 (residues 66-120), and helix 6-7 (residues 143-184). The helix 6-7 segment adopts the same conformation and interactions with the other helical segments of the bundle as helix 6-7 of the symmetry-related molecule in the dimer

structure through a domain swap mechanism in which the helix 5 region (residues 121-142) acts as the flexible hinge. The C-terminal domain encompassing residues 185-243 is a less organized extended structure domain with a little AαH structure, presumably helix 10 (residues 220-241) at the end. Helix 10 was suggested to be an AαH in solution and with a high exclusion pressure on an egg POPC/A/W interface

(27, 29, 58, 66). The domain distributions of the three proteins are illustrated in Fig. 6A. The predicted monomer structures in solution of the three proteins are illustrated in Fig. 6B. In the model of the Δ(1-59)(185-243)apoA-I monomer in solution (Fig. 6B), the deleted residues 1-59 are colored in transparent gray illustrating that there is unlikely to be a tightly packed N-terminal α-helical domain in this protein and some of the hydrophobic residues are exposed.

In our study, full-length apoA-I and Δ(1-59)(185-243) apoA-I show similar adsorption behaviors on both TO/W and POPC/TO/W interfaces. They bind to both interfaces much faster and lower the γ significantly to stabilize the interfaces. Δ(185-243)apoA-I has a relatively slow adsorption rate and lowers the γ less (Fig. 1). These results are consistent with the Π_{EX} data at the POPC/TO/W interface (Fig. 2B), which clearly shows that apoA-I and Δ(1-59)(185-243)apoA-I penetrate into the interface more easily. The slow and weak binding of Δ(185-243)apoA-I to the TO/W and the POPC/TO/W interfaces may indicate that the missing C-terminal 185-243 residues (Fig. 6B) are important in initiating the lipid binding of apoA-I. However additional features must be key to the slow binding because Δ(1-59) (185-243)apoA-I has no C-terminal residues 185-243, but binds rapidly and strongly. It is reasonable to speculate that because Δ(185-243)apoA-I forms a well-packed independent domain (Fig. 6B), it needs more energy and time to open the α-helical bundle to expose its hydrophobic residues to favorably bind to the hydrophobic lipid interface, or it needs to be pulled closer to the interface to open up and bind as would occur if the C-terminal domain was attached. For the full-length apoA-I, a segment of the extended less organized C-terminal domain (residues 185-243), probably the most hydrophobic sequence residues 220-241 (27), may bind to the interface initiating lipid binding. This binding would be followed by the binding of the whole C-terminal region and the formation of a more AαH structure. In this way, the N-terminal bundle may be positioned close to the surface, which finally triggers the opening of the N-terminal bundle exposing the hydrophobic interface, and the whole molecule is bound quickly. Δ(1-59)(185-243)apoA-I shows a similar fast binding as full-length apoA-I but the mechanism is different. Because Δ(1-59)(185-243)apoA-I does not have the N-terminal 1-59 residues that form the tight N-terminal α-helix bundle (Fig. 6B), some of the hydrophobic central residues are exposed and can bind to the hydrophobic interface and lower the γ rapidly. Mei and Atkinson (unpublished observations) have shown that the 1-anilinonaphthalene-8-sulfonate (ANS) fluorescence signal of Δ(1-59)(185-243) apoA-I is higher than that of WT apoA-I and Δ(185-243) apoA-I, suggesting that Δ(1-59)(185-243)apoA-I has more exposed hydrophobic areas. These results are consistent with previous ANS binding experiments (35, 67), which have demonstrated that there is an increase in hydrophobic surface when the N-terminal region of apoA-I is disrupted. A major increase in ANS binding has been shown in the N-terminal truncated Δ(1-43)apoA-I compared with the WT apoA-I, and disruption of the N-terminal region by proline mutagenesis increases the hydrophobic exposure and ANS binding. Therefore, in the absence of the C-terminal 185-243 residues, the opening of the N-terminal α-helix bundle is the rate controlling step for lipid binding. As shown by the structure model (Fig. 6B), the N-terminal 1-59 residues are very important to maintain the N-terminal α-helix bundle conformation. Our results suggest that destabilizing the helical bundle restores the rapid lipid binding. While Δ(185-243)apoA-I is more stable in solution, and Δ(1-59) (185-243)apoA-I favors the interface, the full-length apoA-I has the flexibility to adapt in both environments.

Δ(185-243)apoA-I has slower kinetics and lowers the interfacial tension less compared with the full-length apoA-I and Δ(1-59)(185-243)apoA-I when adsorbed to the TO/W and the POPC/TO/W interfaces (Fig. 1). However, once bound to the interfaces, Δ(185-243)apoA-I displays a desorption behavior similar to apoA-I, but Δ(1-59)(185-243) apoA-I behaves differently. At the TO/W interface, apoA-I and Δ(185-243)apoA-I desorb at similar higher Π_{MAX}s of 17.5 and 17.4 mN/m, respectively, but Δ(1-59)(185-243) apoA-I desorbs at a lower Π_{MAX} of 16.5 mN/m (Fig. 3B). At the POPC/TO/W interface, the Πs at which the proteins desorb depends on the POPC/protein ratio at the interface (Fig. 4). The higher POPC/protein ratio requires higher Πs to eject the proteins. At similar POPC/protein ratios, apoA-I and Δ(185-243)apoA-I are ejected from the POPC/TO/W interface at higher Πs than Δ(1-59)(185-243)apoA-I (Fig. 4D). Thus Δ(1-59)(185-243)apoA-I is an "easy on and easy off" protein.

Several studies suggest that different α-helical domains in apoA-I have different lipid binding abilities (27, 38). Phillips' group measured the Π_es of eight synthesized tandem repeating 22-mer domains of apoA-I at an egg POPC/A/W interface (27) and showed that among the 22-mers, the N- and C-terminal peptides (44-65 and 220-241) exhibited the highest Π_es (28 mN/m and 30 mN/m, respectively) indicating higher affinity to egg POPC. Other central peptides exhibited lower Π_e values (<23 mN/m) indicating lower affinity. We have shown (38) that part of apoA-I can be pushed off the TO/W interface at low pressure (∼15 mN/m), while the full-length apoA-I is ejected from the interface at a much higher pressure (∼19 mN/m). Compared with Δ(1-59)(185-243)apoA-I, Δ(185-243)apoA-I contains a strong lipid binding domain (residues 44-65). Once bound, Δ(185-243)apoA-I associates with the lipid more strongly. Δ(1-59) (185-243)apoA-I contains only the central α-helical domains with weak lipid binding affinity, so it desorbs much more easily at lower Πs.

That Δ(185-243)apoA-I displays a slow kinetic on adsorption, but a strong surface stability during desorption, suggests that the binding of Δ(185-243)apoA-I to the lipid interface involves a significant conformational change including the opening of the N-terminal α-helical bundle. The opening of the N-terminal α-helical bundle is the rate-controlling step, slowing the adsorption of Δ(185-243) apoA-I. On the other hand, once bound, the N-terminal helices in residues 1-59 are bound and desorption of the protein is controlled by the strong lipid affinity of the α-helical domains, probably in the N-terminal residues 44-65, which anchor the protein more strongly. Thus Δ(185-243) apoA-I is a "hard on and hard off" protein.

In addition, our sequential slow expansion and compression experiments on the POPC/TO/W interface suggest some desorption details in terms of partial desorption (Fig. 5). Only part of apoA-I desorbs at Πs below 22 mN/m. The whole apoA-I molecule desorbs at Πs above 22 mN/m as indicated by the Π_E (Fig. 5D). Part of $\Delta(185\text{-}243)$apoA-I desorbs at Πs below 23.5 mN/m, and the whole protein molecule desorbs at higher Πs (Fig. 5C). $\Delta(1\text{-}59)(185\text{-}243)$apoA-I does not show a partial desorption at lower Πs, instead the whole protein molecule is ejected at around 21 mN/m at the lowest POPC/protein ratio (the starting ratio). $\Delta(1\text{-}59)(185\text{-}243)$ is missing the exon 3 encoded N-terminal residues 1-43. Previous studies in our lab (53, 58) have shown that a synthesized N-terminal peptide of apoA-I encompassing residues 1-44 has a weaker lipid binding affinity at both the TO/W and the POPC/TO/W interfaces, compared with a C-terminal peptide encompassing residues 198-243. In fact when equal amounts of the N-terminal peptide (residues 1-44) and the C-terminal peptide (residues 198-243) were added to the aqueous phase surrounding a TO/W interface, they both adsorbed on the interface but the C-terminal peptide (residues 198-243) gradually pushed off the N-terminal peptide (residues 1-44) to leave only the C-terminal peptide (residues 198-243) on the interface (58). We speculate that once bound to the POPC/TO/W interface, the N-terminal 1-43 residues are the first region to be ejected at relatively lower Πs. This region readsorbs quickly upon reexpansion. $\Delta(1\text{-}59)(185\text{-}243)$ lacks this domain and the sequences encompassing residues 44-65 and 220-241 supposed to have strong lipid binding ability (27), and this protein maintains an average moderate lipid binding affinity. Thus, it desorbs from the POPC/TO/W interface more like a whole unit without showing any partial desorption behavior.

All three proteins bind to the POPC/TO/W interface faster than to the TO/W interface, as shown by the absence of a lag phase in the adsorption isotherms, and the equilibrium γ is much lower at the same protein concentration (Fig. 1); whereas, bound proteins desorb from the POPC/TO/W interface at much higher surface pressures (Fig. 4D). Thus POPC molecules enhance the lipid binding and the protein stability on the interface. We suggest that, in addition to the interaction between the protein and the core lipids, the protein has a much stronger interaction with POPC molecules. It is possible that POPC aids the opening of the N-terminal domain. In the N-terminal α-helix bundle, there is an opening between the extended region formed by helix 1 and the body of the bundle at the N-terminal end (19), through which the POPC molecules might contact the hydrophobic core of the bundle and assist the opening and unhinging of the bundle.

The well-established two step lipid binding mechanism model (18, 27) concerning the conformational changes when apoA-I adsorbs to the lipoprotein surface suggests that the C-terminal domain of lipid-free apoA-I initiates the lipid binding, and subsequently the N-terminal helical bundle domain undergoes a conformational unhinging to open to bind to lipid. Our present study focuses on the lipid association of apoA-I with spherical lipoprotein particles and the conformational changes involved in the adsorption and desorption when apoA-I exchanges among different lipoprotein particles. In our previous studies (38) of the interfacial behavior of apoA-I and a consensus sequence peptide at the TO/W interface, we proposed a model for the adsorption and desorption of apoA-I onto a spherical lipoprotein particle. The main concept is that apoA-I binds to the lipoprotein particle rapidly to stabilize the lipoprotein surface efficiently, and because different domains of apoA-I have different lipid binding affinity, they desorb at different pressures. Our present study further shows that different domains of apoA-I play different roles in lipid binding (**Fig. 7**). Regions in the C-terminal domain (residues 185-243), and presumably helix 10 (residues 221-242) with the highest exclusion pressure (27), are important to initiate the lipid binding (step 1 in Fig. 7). This interaction triggers the opening of the adjacent N-terminal α-helical bundle to convert the hydrophobic interactions between the α-helices to helix-lipid interactions at the interface (steps 2 and 3 in Fig. 7). During the opening of the N-terminal α-helical bundle, the flexible hinge regions, helix 5 (residues 121-142), residues 35-43, and the loop region (residues 65-68), unhinge and the protein spreads on the interface. On desorption, different domains of apoA-I desorb in a sequential order depending on their different lipid binding affinity. The N-terminal 1-43 residues presumably desorb first at very low surface pressure followed by the central domains, with the exception of residues 44-65 and 221-243. Finally these most strongly bound segments desorb and the apoA-I molecule refolds in the solution [steps 4, 6, and 8 in Fig. 7]. When the interface re-expands to the original state [steps 7 and 5 in Fig. 7], because apoA-I is still anchored on the interface, the ejected part of apoA-I readsorbs on the interface rapidly.

In a hydrogen exchange and mass spectrometry study of the helical structure and the stability of apoA-I in discoidal HDL particles, Chetty et al. (37) have shown that the apoA-I molecule incorporated around the edge of small HDL particles (7.8 nm) has 20% more residues out of direct contact with the phospholipids than in larger HDL particles (9.6 nm) due to the increase in packing density of the protein. These detached segments form disordered loops and are the same segments that form loops in the lipid-free state. In our study, when apoA-I partially or fully desorbs from the model lipoprotein interface (steps 4, 6 and 8 in Fig. 7) at certain threshold pressures, we speculate that the desorption reverses the corresponding adsorption process, and the conformational changes are reversible too. As shown in step 4 of Fig. 7, the N-terminal sub-domain (residues 1-43) and the central segments, except the two strong lipid binding regions (residues 44-65 and 221-243), are detached from the interface forming either helical or extended structures as they were previously in solution; in step 6 of Fig. 7, residues 44-65 are detached from the interface and the entire α-helical bundle refolds; and in step 8 of Fig. 7, residues 221-242 are detached eventually and the entire apoA-I molecule refolds in solution.

During lipid metabolism, apoA-I adsorbs on, partially or fully desorbs from, and exchanges among different lipoproteins in the plasma to fulfill its multiple functions. On one hand, apoA-I binds to lipoproteins to modify the surface
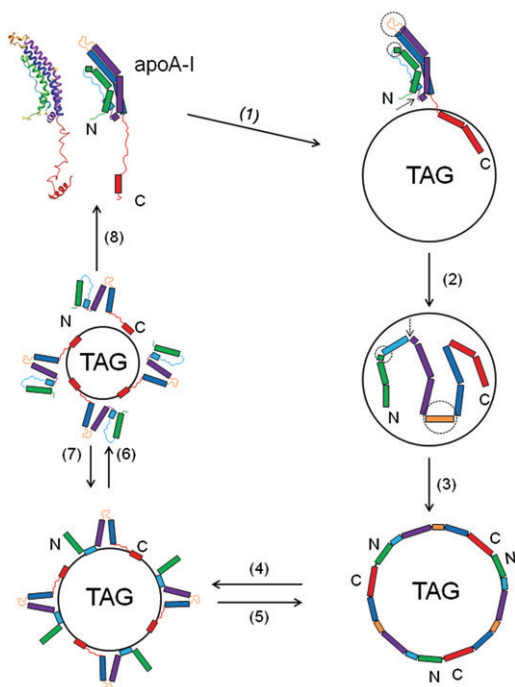
Fig. 7. A schematic model for the adsorption and desorption behaviors of apoA-I on the TO/W interface. Step 1 (1): The adsorption of lipid-free apoA-I to the TO/W interface is initiated by the binding of some sequences in the C-terminal domain, presumably the sequence between residues 220 and 243; then the whole C-terminal domain binds forming the AαH domain and pulls the N-terminal α-helical bundle into close proximity to the TO/W interface. The flexible hinge regions in the N-terminal α-helical bundle are indicated by dashed circles (residues 35-43 and 121-142) and pointed to by a dashed arrow (residues 65-68). Step 2 (2): The hinge regions unhinge and the N-terminal α-helical bundle opens up and binds to the interface. Upon binding the helix 5 region (residues 121-142) changes its structure from a loop to an AαH structure. Some loop regions, like the sequence between residues 44 and 55, may also form AαH structures. Step 3 (3): Once the interface is saturated by apoA-I molecules, it reaches equilibrium. The protein is fully spread on the surface with most, if not all, of the AαHs engaged in the TO/W interface. Step 4 (4): Small decreases in the surface area give rise to small increases in surface pressure. When the surface pressure goes above a threshold pressure (∼15 mN/m) (38), conformational changes occur in apoA-I, which allow some portion of the apoA-I to disassociate from the TO/W interface leaving the strong lipid binding regions of the protein, presumably helix 1 (residues 44-65) and helix 10 (residues 220-243), attached. Step 5 (5): If the area is suddenly restored to the original area, then these portions rapidly snap back onto the surface. Step 6 (6): Further compression ejects more regions of apoA-I from the surface, probably only the helix 10 region remains on the surface. Step 7 (7): Reversible readsorption occurs when the surface is expanded back to the previous state. Step 8 (8): If the area of the droplet is decreased to increase the surface pressure to above ∼19 mN/m (48), then the entire protein disassociates into the aqueous phase and refolds. Once some apoA-I desorbs, the surface pressure relaxes and some apoA-I remains on the surface. Most of the apoA-I will desorb only if the pressure continues to increase, i.e., the area available continues to decrease.

for enzyme reactions, receptor binding, or lipid transfer activities; on the other hand, lipoprotein particles constantly change in size, shape, and composition as a result of enzyme reactions and lipid transfer activities. Surface pressure changes are likely to occur during all these remodeling and reactions. ApoA-I is a very flexible protein in that it adopts a structure similar to the molten globular state (68). The multiple AαHs in apoA-I exhibit stabilization free energies in the range of 3–5 kcal/mol indicating high flexibility and dynamic folding and refolding in seconds (37, 66). Thus apoA-I is very sensitive to changes in the environment, i.e., the size, shape, composition, and most importantly the surface pressure changes of the lipoprotein particle with which it associates. The surface pressure changes in HDL also probably trigger the conformational reorganization, induce the conformational changes, and even desorption of apoA-I from HDL.

The surface pressure changes maybe transient or more long-term. For instance, newly secreted TAG-rich lipoproteins (CMs and VLDLs) have low cholesterol/PL ratios. They take up cholesterol when they enter the plasma. The surface pressure will gradually increase as cholesterol in the surface takes up more space and pushes the surface molecules closer together. In addition, nascent CM absorbs certain soluble apolipoproteins from plasma, e.g., apoCs and apoA-I, rapidly increasing the surface pressure. When the surface pressure increases, all lipoprotein surface components are pushed together, i.e., the area per molecule decreases. As a result, some loosely bound lipids, like short- to mid-chain fatty acids, may desorb, and also lightly bound apolipoproteins like apoA-IV (which is secreted with CM) come off rapidly once in plasma. Thus, the circulating plasma CM has a different surface composition and pressure than the nascent CM. The higher surface pressure can cause some apolipoproteins to desorb into plasma or cause others to change their surface conformation. Some enzymes in the plasma also act on the surface of CM. Lipoprotein lipase and its cofactor apoC-2 bind to the interface and hydrolyze TAG to half ionized fatty acids and 2-monoacylglycerol. They are strongly surface active and go to the surface, transiently increasing the surface pressure further. As core TAG is depleted the core shrinks which, unless the surface is distorted from its spherical shape, will further increase the surface pressure to a potentially high level. Apolipoproteins at the surface sense this high lateral force placed on them and those weakly bound apolipoproteins desorb. Complex apolipoproteins like apoA-I (and apoB) stay partly bound by domains with higher surface affinity desorbing loosely bound domains into the adjacent aqueous phase. These changes would decrease the surface area of apolipoproteins and stabilize or buffer the surface pressure in the short term. But, as lipoprotein lipase continues to hydrolyze, TAG pressure would rise again. Some relief from high pressure will occur as albumin removes fatty acids and perhaps 2-monoacylglycerol from the interface. Note that apoB is irreversibly bound to CM and VLDL by its amphipathic β strand domains (60), whereas its other loosely bound domains can desorb, thus decreasing the area covered by apoB (62). These detached domains probably have an altered conformation and perhaps change their ligand binding properties.

Many other enzymatic/transfer proteins in plasma can alter the surface pressure. For example, removal of phospholipids from the lipoprotein surface by phospholipases

or phospholipid transfer protein could lower surface pressure. On the other hand cholesteryl ester transfer protein could decrease the core volume and increase the surface pressure by exchanging a large molecule (TAG, volume is ~ 1460 Å^3) for a smaller CE molecule (~ 1140 Å^3) (69). Increasing the surface pressure has many effects. It can desorb weakly bound apolipoproteins and lipids, change apolipoprotein conformation in weakly bound domains making them ligands for other interactions, change the surface density of the lipid monolayer, and force the surface located TAG (and CE) back into the core. Therefore, we speculate that the surface interaction, adsorption, and desorption of apolipoproteins at the lipoprotein surfaces, and the actions of enzymes and transfer proteins all work together to modulate the surface pressure and composition to potentially alter the conformation and reactivity of apolipoproteins at the surface. HDL is a target for LCAT, cholesteryl ester transfer protein, phospholipid transfer protein, hepatic lipase, and endothelial lipase. The surface pressure of HDL changes during HDL remodeling and enzyme reactions. The conformational reorganization of apoA-I enables it to stabilize HDL particles, and to interact with enzymes, receptors, and lipid transfer proteins. A large number of conformational states can exist between fully (all helices) bound and unbound. These include the partly adsorbed and partly ejected states where the ejected part(s) may have a specific conformation necessary for binding to a cofactor, ABC transporter, lipid transfer protein, or apolipoprotein receptor. Furthermore, the different lipid association abilities of different domains and the cooperativity of different domains make apoA-I a very elastic and flexible protein, so that it can easily unfold and refold to adapt to different environments. Diverse conformations of apoA-I also allow it to act as either labile for exchange or stable on the lipoprotein surface to help maintain the lipoprotein structure. We suggest that during lipoprotein remodeling, surface pressure-mediated adsorption, partial or full desorption, and readsorption underlie the conformational flexibility of apoA-I, which allows apoA-I exchange among different lipoproteins and facilitates its multiple functions.

REFERENCES

1. Castelli, W. P., J. T. Doyle, T. Gordon, C. G. Hames, M. C. Hjortland, S. B. Hulley, A. Kagan, and W. J. Zukel. 1977. HDL cholesterol and other lipids in coronary heart disease. The cooperative lipoprotein phenotyping study. *Circulation.* **55:** 767–772.
2. Fielding, C. J., and P. E. Fielding. 1995. Molecular physiology of reverse cholesterol transport. *J. Lipid Res.* **36:** 211–228.
3. Rye, K. A., and P. J. Barter. 2004. Formation and metabolism of prebeta-migrating, lipid-poor apolipoprotein A-I. *Arterioscler. Thromb. Vasc. Biol.* **24:** 421–428.
4. Tall, A. R. 1998. An overview of reverse cholesterol transport. *Eur. Heart J.* **19(Suppl A):** A31–A35.
5. Atkinson, D., and D. M. Small. 1986. Recombinant lipoproteins: implications for structure and assembly of native lipoproteins. *Annu. Rev. Biophys. Biophys. Chem.* **15:** 403–456.
6. Gursky, O. 2013. Crystal structure of Δ(185-243)ApoA-I suggests a mechanistic framework for the protein adaptation to the changing lipid load in good cholesterol: from flatland to sphereland via double belt, belt buckle, double hairpin and trefoil/tetrafoil. *J. Mol. Biol.* **425:** 1–16.
7. Segrest, J. P., M. K. Jones, A. E. Klon, C. J. Sheldahl, M. Hellinger, H. De Loof, and S. C. Harvey. 1999. A detailed molecular belt model for apolipoprotein A-I in discoidal high density lipoprotein. *J. Biol. Chem.* **274:** 31755–31758.
8. Silva, R. A., R. Huang, J. Morris, J. Fang, E. O. Gracheva, G. Ren, A. Kontush, W. G. Jerome, K. A. Rye, and W. S. Davidson. 2008. Structure of apolipoprotein A-I in spherical high density lipoproteins of different sizes. *Proc. Natl. Acad. Sci. USA.* **105:** 12176–12181.
9. Segrest, J. P., R. L. Jackson, J. D. Morrisett, and A. M. Gotto, Jr. 1974. A molecular theory of lipid-protein interactions in the plasma lipoproteins. *FEBS Lett.* **38:** 247–258.
10. Segrest, J. P., M. K. Jones, H. De Loof, C. G. Brouillette, Y. V. Venkatachalapathi, and G. M. Anantharamaiah. 1992. The amphipathic helix in the exchangeable apolipoproteins: a review of secondary structure and function. *J. Lipid Res.* **33:** 141–166.
11. Fang, Y., O. Gursky, and D. Atkinson. 2003. Lipid-binding studies of human apolipoprotein A-I and its terminally truncated mutants. *Biochemistry.* **42:** 13260–13268.
12. Fang, Y., O. Gursky, and D. Atkinson. 2003. Structural studies of N- and C-terminally truncated human apolipoprotein A-I. *Biochemistry.* **42:** 6881–6890.
13. Gorshkova, I. N., K. Liadaki, O. Gursky, D. Atkinson, and V. I. Zannis. 2000. Probing the lipid-free structure and stability of apolipoprotein A-I by mutation. *Biochemistry.* **39:** 15910–15919.
14. Gorshkova, I. N., T. Liu, V. I. Zannis, and D. Atkinson. 2002. Lipid-free structure and stability of apolipoprotein A-I: probing the central region by mutation. *Biochemistry.* **41:** 10529–10539.
15. Laccotripe, M., S. C. Makrides, A. Jonas, and V. I. Zannis. 1997. The carboxyl-terminal hydrophobic residues of apolipoprotein A-I affect its rate of phospholipid binding and its association with high density lipoprotein. *J. Biol. Chem.* **272:** 17511–17522.
16. Rogers, D. P., L. M. Roberts, J. Lebowitz, J. A. Engler, and C. G. Brouillette. 1998. Structural analysis of apolipoprotein A-I: effects of amino- and carboxy-terminal deletions on the lipid-free structure. *Biochemistry.* **37:** 945–955.
17. Saito, H., P. Dhanasekaran, D. Nguyen, P. Holvoet, S. Lund-Katz, and M. C. Phillips. 2003. Domain structure and lipid interaction in human apolipoproteins A-I and E, a general model. *J. Biol. Chem.* **278:** 23227–23232.
18. Saito, H., S. Lund-Katz, and M. C. Phillips. 2004. Contributions of domain structure and lipid interaction to the functionality of exchangeable human apolipoproteins. *Prog. Lipid Res.* **43:** 350–380.
19. Mei, X., and D. Atkinson. 2011. Crystal structure of C-terminal truncated apolipoprotein A-I reveals the assembly of high density lipoprotein (HDL) by dimerization. *J. Biol. Chem.* **286:** 38570–38582.
20. Brouillette, C. G., and G. M. Anantharamaiah. 1995. Structural models of human apolipoprotein A-I. *Biochim. Biophys. Acta.* **1256:** 103–129.
21. Brouillette, C. G., G. M. Anantharamaiah, J. A. Engler, and D. W. Borhani. 2001. Structural models of human apolipoprotein A-I: a critical analysis and review. *Biochim. Biophys. Acta.* **1531:** 4–46.
22. Pittman, R. C., C. K. Glass, D. Atkinson, and D. M. Small. 1987. Synthetic high density lipoprotein particles. Application to studies of the apoprotein specificity for selective uptake of cholesterol esters. *J. Biol. Chem.* **262:** 2435–2442.
23. Pownall, H. J., J. B. Massey, S. K. Kusserow, and A. M. Gotto, Jr. 1979. Kinetics of lipid–protein interactions: effect of cholesterol on the association of human plasma high-density apolipoprotein A-I with L-alpha-dimyristoylphosphatidylcholine. *Biochemistry.* **18:** 574–579.
24. Ritter, M. C., and A. M. Scanu. 1977. Role of apolipoprotein A-I in the structure of human serum high density lipoproteins. Reconstitution studies. *J. Biol. Chem.* **252:** 1208–1216.
25. Scanu, A. M. 1972. Structural studies on serum lipoproteins. *Biochim. Biophys. Acta.* **265:** 471–508.
26. Tall, A. R., D. M. Small, R. J. Deckelbaum, and G. G. Shipley. 1977. Structure and thermodynamic properties of high density lipoprotein recombinants. *J. Biol. Chem.* **252:** 4701–4711.
27. Palgunachari, M. N., V. K. Mishra, S. Lund-Katz, M. C. Phillips, S. O. Adeyeye, S. Alluri, G. M. Anantharamaiah, and J. P. Segrest. 1996. Only the two end helixes of eight tandem amphipathic helical domains of human apo A-I have significant lipid affinity. Implications for HDL assembly. *Arterioscler. Thromb. Vasc. Biol.* **16:** 328–338.
28. Zhu, H. L., and D. Atkinson. 2004. Conformation and lipid binding of the N-terminal (1–44) domain of human apolipoprotein A-I. *Biochemistry.* **43:** 13156–13164.
29. Zhu, H. L., and D. Atkinson. 2007. Conformation and lipid binding of a C-terminal (198–243) peptide of human apolipoprotein A-I. *Biochemistry.* **46:** 1624–1634.

30. Chao, Y. 2002. Conformational Studies of a Consensus Sequence Peptide (CSP) and a Real Sequence Peptide (RSP) of Apolipoproteins by Circular Dichroism and X-ray Crystallography. PhD Dissertation. Boston University School of Medicine, Boston, MA.

31. Narayanaswami, V., and R. O. Ryan. 2000. Molecular basis of exchangeable apolipoprotein function. *Biochim. Biophys. Acta.* **1483:** 15–36.

32. Davidson, W. S., T. Hazlett, W. W. Mantulin, and A. Jonas. 1996. The role of apolipoprotein AI domains in lipid binding. *Proc. Natl. Acad. Sci. USA.* **93:** 13605–13610.

33. Saito, H., P. Dhanasekaran, D. Nguyen, E. Deridder, P. Holvoet, S. Lund-Katz, and M. C. Phillips. 2004. Alpha-helix formation is required for high affinity binding of human apolipoprotein A-I to lipids. *J. Biol. Chem.* **279:** 20974–20981.

34. Mishra, V. K., M. N. Palgunachari, G. Datta, M. C. Phillips, S. Lund-Katz, S. O. Adeyeye, J. P. Segrest, and G. M. Anantharamaiah. 1998. Studies of synthetic peptides of human apolipoprotein A-I containing tandem amphipathic alpha-helixes. *Biochemistry.* **37:** 10313–10324.

35. Tanaka, M., P. Dhanasekaran, D. Nguyen, S. Ohta, S. Lund-Katz, M. C. Phillips, and H. Saito. 2006. Contributions of the N- and C-terminal helical segments to the lipid-free structure and lipid interaction of apolipoprotein A-I. *Biochemistry.* **45:** 10351–10358.

36. Kono, M., Y. Okumura, M. Tanaka, D. Nguyen, P. Dhanasekaran, S. Lund-Katz, M. C. Phillips, and H. Saito. 2008. Conformational flexibility of the N-terminal domain of apolipoprotein a-I bound to spherical lipid particles. *Biochemistry.* **47:** 11340–11347.

37. Sevugan Chetty, P., L. Mayne, Z. Y. Kan, S. Lund-Katz, S. W. Englander, and M. C. Phillips. 2012. Apolipoprotein A-I helical structure and stability in discoidal high-density lipoprotein (HDL) particles by hydrogen exchange and mass spectrometry. *Proc. Natl. Acad. Sci. USA.* **109:** 11687–11692.

38. Wang, L., D. Atkinson, and D. M. Small. 2005. The interfacial properties of ApoA-I and an amphipathic alpha-helix consensus peptide of exchangeable apolipoproteins at the triolein/water interface. *J. Biol. Chem.* **280:** 4154–4165.

39. Cavigiolio, G., B. Shao, E. G. Geier, G. Ren, J. W. Heinecke, and M. N. Oda. 2008. The interplay between size, morphology, stability, and functionality of high-density lipoprotein subclasses. *Biochemistry.* **47:** 4770–4779.

40. Masson, D., X. C. Jiang, L. Lagrost, and A. R. Tall. 2009. The role of plasma lipid transfer proteins in lipoprotein metabolism and atherogenesis. *J. Lipid Res.* **50(Suppl):** S201–S206.

41. Rye, K. A., C. A. Bursill, G. Lambert, F. Tabet, and P. J. Barter. 2009. The metabolism and anti-atherogenic properties of HDL. *J. Lipid Res.* **50(Suppl):** S195–S200.

42. Small, D. M., and M. C. Phillips. 1992. A technique to estimate the apparent surface pressure of emulsion particles using apolipoproteins as probes. *Adv. Colloid Interface Sci.* **41:** 1–8.

43. Datta, G., M. Chaddha, S. Hama, M. Navab, A. M. Fogelman, D. W. Garber, V. K. Mishra, R. M. Epand, R. F. Epand, S. Lund-Katz, et al. 2001. Effects of increasing hydrophobicity on the physical-chemical and biological properties of a class A amphipathic helical peptide. *J. Lipid Res.* **42:** 1096–1104.

44. Ibdah, J. A., K. E. Krebs, and M. C. Phillips. 1989. The surface properties of apolipoproteins A-I and A-II at the lipid/water interface. *Biochim. Biophys. Acta.* **1004:** 300–308.

45. Ibdah, J. A., S. Lund-Katz, and M. C. Phillips. 1989. Molecular packing of high-density and low-density lipoprotein surface lipids and apolipoprotein A-I binding. *Biochemistry.* **28:** 1126–1133.

46. Ibdah, J. A., and M. C. Phillips. 1988. Effects of lipid composition and packing on the adsorption of apolipoprotein A-I to lipid monolayers. *Biochemistry.* **27:** 7155–7162.

47. Krebs, K. E., J. A. Ibdah, and M. C. Phillips. 1988. A comparison of the surface activities of human apolipoproteins A-I and A-II at the air/water interface. *Biochim. Biophys. Acta.* **959:** 229–237.

48. Phillips, M. C., and K. E. Krebs. 1986. Studies of apolipoproteins at the air-water interface. *Methods Enzymol.* **128:** 387–403.

49. Weinberg, R. B., V. R. Cook, J. A. DeLozier, and G. S. Shelness. 2000. Dynamic interfacial properties of human apolipoproteins A-IV and B-17 at the air/water and oil/water interface. *J. Lipid Res.* **41:** 1419–1427.

50. Weinberg, R. B., J. A. Ibdah, and M. C. Phillips. 1992. Adsorption of apolipoprotein A-IV to phospholipid monolayers spread at the air/water interface. A model for its labile binding to high density lipoproteins. *J. Biol. Chem.* **267:** 8977–8983.

51. Meyers, N. L., L. Wang, O. Gursky, and D. M. Small. 2013. Changes in helical content or net charge of apolipoprotein C-I alter its affinity for lipid/water interfaces. *J. Lipid Res.* **54:** 1927–1938.

52. Meyers, N. L., L. Wang, and D. M. Small. 2012. Apolipoprotein C-I binds more strongly to phospholipid/triolein/water than triolein/water interfaces: a possible model for inhibiting cholesterol ester transfer protein activity and triacylglycerol-rich lipoprotein uptake. *Biochemistry.* **51:** 1238–1248.

53. Mitsche, M. A., and D. M. Small. 2011. C-terminus of apolipoprotein A-I removes phospholipids from a triolein/phospholipids/water interface, but the N-terminus does not: a possible mechanism for nascent HDL assembly. *Biophys. J.* **101:** 353–361.

54. Mitsche, M. A., and D. M. Small. 2013. Surface pressure-dependent conformation change of apolipoprotein-derived amphipathic alpha-helices. *J. Lipid Res.* **54:** 1578–1588.

55. Mitsche, M. A., L. Wang, Z. G. Jiang, C. J. McKnight, and D. M. Small. 2009. Interfacial properties of a complex multi-domain 490 amino acid peptide derived from apolipoprotein B (residues 292-782). *Langmuir.* **25:** 2322–2330.

56. Small, D. M., L. Wang, and M. A. Mitsche. 2009. The adsorption of biological peptides and proteins at the oil/water interface. A potentially important but largely unexplored field. *J. Lipid Res.* **50(Suppl):** S329–S334.

57. Wang, L., D. Atkinson, and D. M. Small. 2003. Interfacial properties of an amphipathic alpha-helix consensus peptide of exchangeable apolipoproteins at air/water and oil/water interfaces. *J. Biol. Chem.* **278:** 37480–37491.

58. Wang, L., N. Hua, D. Atkinson, and D. M. Small. 2007. The N-terminal (1-44) and C-terminal (198-243) peptides of apolipoprotein A-I behave differently at the triolein/water interface. *Biochemistry.* **46:** 12140–12151.

59. Wang, L., Z. G. Jiang, C. J. McKnight, and D. M. Small. 2010. Interfacial properties of apolipoprotein B292-593 (B6.4-13) and B611-782 (B13-17). Insights into the structure of the lipovitellin homology region in apolipoprotein B. *Biochemistry.* **49:** 3898–3907.

60. Wang, L., D. D. Martin, E. Genter, J. Wang, R. S. McLeod, and D. M. Small. 2009. Surface study of apoB1694-1880, a sequence that can anchor apoB to lipoproteins and make it nonexchangeable. *J. Lipid Res.* **50:** 1340–1352.

61. Wang, L., and D. M. Small. 2004. Interfacial properties of amphipathic beta strand consensus peptides of apolipoprotein B at oil/water interfaces. *J. Lipid Res.* **45:** 1704–1715.

62. Wang, L., M. T. Walsh, and D. M. Small. 2006. Apolipoprotein B is conformationally flexible but anchored at a triolein/water interface: a possible model for lipoprotein surfaces. *Proc. Natl. Acad. Sci. USA.* **103:** 6871–6876.

63. Wetterau, J. R., and A. Jonas. 1982. Effect of dipalmitoylphosphatidylcholine vesicle curvature on the reaction with human apolipoprotein A-I. *J. Biol. Chem.* **257:** 10961–10966.

64. Labourdenne, S., N. Gaudry-Rolland, S. Letellier, M. Lin, A. Cagna, G. Esposito, R. Verger, and C. Rivière. 1994. The oil-drop tensiometer: potential applications for studying the kinetics of (phospho) lipase action. *Chem. Phys. Lipids.* **71:** 163–173.

65. Mitsche, M. A., L. Wang, and D. M. Small. 2010. Adsorption of egg phosphatidylcholine to an air/water and triolein/water bubble interface: use of the 2-dimensional phase rule to estimate the surface composition of a phospholipid/triolein/water surface as a function of surface pressure. *J. Phys. Chem. B.* **114:** 3276–3284.

66. Chetty, P. S., L. Mayne, S. Lund-Katz, D. Stranz, S. W. Englander, and M. C. Phillips. 2009. Helical structure and stability in human apolipoprotein A-I by hydrogen exchange and mass spectrometry. *Proc. Natl. Acad. Sci. USA.* **106:** 19005–19010.

67. Rogers, D. P., C. G. Brouillette, J. A. Engler, S. W. Tendian, L. Roberts, V. K. Mishra, G. M. Anantharamaiah, S. Lund-Katz, M. C. Phillips, and M. J. Ray. 1997. Truncation of the amino terminus of human apolipoprotein A-I substantially alters only the lipid-free conformation. *Biochemistry.* **36:** 288–300.

68. Gursky, O., and D. Atkinson. 1996. Thermal unfolding of human high-density apolipoprotein A-1: implications for a lipid-free molten globular state. *Proc. Natl. Acad. Sci. USA.* **93:** 2991–2995.

69. Small, D. M. 1986. The Physical Chemistry of Lipids. From Alkanes to Phospholipids. Plenum Press, New York